Numerical Heat Transfer, Part A, 36:327–344, 1999

1040–7782/99 $12.00+ .00

NONSIMILAR HYDROMAGNETIC SIMULTANEOUS HEAT AND MASS TRANSFER BY MIXED CONVECTION FROM A VERTICAL PLATE EMBEDDED IN A UNIFORM POROUS MEDIUM

Ali J. Chamkha and Abdul-Rahim A. Khaled
Department of Mechanical and Industrial Engineering, Kuwait University, P.O. Box 5969, Safat, 13060 Kuwait

This work considers steady, laminar, hydromagnetic simultaneous heat and mass transfer by mixed convection flow over a permeable vertical plate immersed in a uniform porous medium for the cases of power law variations of both the wall temperature and concentration and the wall heat flux and mass flux. Appropriate transformations are employed to transform the governing differential equations to a nonsimilar form. The transformed equations are solved numerically by an accurate, implicit, iterative, finite difference method. The obtained results are validated by favorable comparisons with previously published work on special cases of the problem. A parametric study illustrating the influence of all involved parameters on the local Nusselt and Sherwood numbers is conducted. The results of this parametric study are shown graphically, and the physical aspects of the problem are discussed.

INTRODUCTION

Simultaneous heat and mass transfer from different geometries embedded in porous media has many engineering and geophysical applications, such as migration of water in geothermal reservoirs, underground spreading of chemical wastes and other pollutants, thermal insulation, enhanced oil recovery, packed-bed catalytic reactors, cooling of nuclear reactors, grain storage, and evaporative cooling and solidification [1]. For a flow Reynolds number less than unity, the porous medium can be modeled by the Darcy law, which assumes a linear empirical relation between the Darcian velocity and the pressure drop across the porous medium, as most early authors on porous media have used. However, when the flow velocity in the porous medium is relatively high, inertia and thermal dispersion effects become significant. The high flow velocity is realized when the Reynolds number based on the pore size is greater than unity. The importance of inertia and thermal dispersion effects has been discussed by Vafai and co-workers [2, 3].

Cheng and Minkowycz [4] have presented similarity solutions for free thermal convection from a vertical plate in a fluid-saturated porous medium. The problem of combined thermal convection from a semi-infinite vertical plate in the presence or absence of a porous medium has been studied by many authors [e.g., 5–8]. Nakayama and Koyama [7] have suggested similarity transformations for pure,

Received 12 November 1998, accepted 19 March 1999.
Address correspondence to Professor Ali J. Chamkha, Department of Mechanical and Industrial Engineering, Kuwait University, P.O. Box 5969, Safat, 13060, Kuwait.

NOMENCLATURE

B_0	magnetic field strength	T_w	wall temperature
c_p	fluid specific heat	T_∞	free stream temperature
C	concentration at any point in the flow field	u	tangential or x component of velocity
C_w	concentration at the wall	u_∞	free stream velocity
C_∞	concentration at the free stream	UHF/UMF	uniform wall heat and mass fluxes
D	mass diffusivity		
D_s	porous medium thermal dispersion parameter	v	normal or y component of velocity
f	dimensionless stream function	V_w	wall mass transfer velocity
F	inertia coefficient of the porous medium	V_0	dimensionless wall mass transfer coefficient
g	gravitational acceleration	x	vertical distance along the plate
h	local convective heat transfer coefficient	y	horizontal distance normal to the plate
h_m	local mass transfer coefficient	α	molecular thermal diffusivity of the fluid
k_e	porous medium effective thermal conductivity	α_d	thermal diffusivity of the porous medium due to thermal dispersion
K	permeability of the porous medium		
Le	Lewis number	α_e	effective thermal diffusivity of the porous medium
m	power law index for PHF/PMF		
m_w	wall mass flux	β_C	concentration expansion coefficient
M	square of the Hartmann number		
n	power law index for PST/PSC	β_T	thermal expansion coefficient
N	buoyancy ratio	γ	thermal dispersion constant
Nu_x	local Nusselt number	δ_Q	dimensionless heat generation/absorption parameter (PHF/PMF)
Pe_x	local Péclet number		
PHF/PMF	prescribed wall heat and mass fluxes	δ_T	dimensionless heat generation/ (PST/PSC) bsorption parameter
PST/PSC	prescribed wall temperature and concentration		
q_w	wall heat flux	ϕ	dimensionless concentration
Q_0	heat generation or absorption coefficient	η	coordinate transformation in terms of x and y
Ra_x	local Rayleigh number (PST/PSC)	θ	dimensionless temperature
		ν	fluid kinematic viscosity
Ra_x^*	local Rayleigh number (PHF/PMF)	ξ	mixed convection parameter
		ρ	fluid density
Sh_x	local Sherwood number	σ	fluid electrical conductivity
T	temperature at any point	ψ	stream function

combined, and forced convection in Darcian and non-Darcian porous media. Hsieh et al. [8] have presented nonsimilar solutions for combined convection in porous media. Gorla et al. [9] have studied the effects of free stream thermal stratification and thermal dispersion on combined convection over a vertical plate embedded in a uniform porous medium. Chamkha [10] has investigated hydrodynamic natural convection from an isothermal inclined surface adjacent to a thermally stratified porous medium. Recently, Lai [11] has investigated coupled heat and mass transfer by mixed convection from an isothermal plate embedded in a porous medium. Yih

[12] has studied coupled heat and mass transfer in mixed convection over a vertical plate in a uniform saturated porous medium with prescribed wall temperature and concentration and heat and mass fluxes.

A secondary effect of a porous medium on the flow appears as a result of mixing and recirculation of local fluid particles through tortuous paths formed by the porous medium solid particles. This effect is classified as thermal dispersion (see [3]). Plumb [13] modeled thermal dispersion effects over a vertical plate as linear increases of a fluid thermal diffusivity with increases in the tangential flow velocity. In their model, Amiri and Vafai [3] have shown that the thermal diffusivity of the fluid is also proportional the free stream Reynolds number based on the porous medium pore diameter. Other works dealing with thermal dispersion effects in porous media can be found in the papers by Hong and Tien [14] and Cheng and Vortmeyer [15].

The study of magnetohydrodynamic (MHD) flow and heat transfer in porous and nonporous media is important in applications where a magnetic field is used to control the flow and the performance of many systems using electrically conducting fluids. For example, Rapits et al. [16] have analyzed hydromagnetic free convection flow through a porous medium between two parallel plates. Aldoss et al. [17] have studied mixed convection from a vertical plate embedded in a porous medium in the presence of a magnetic field. Bian et al. [18] have reported on the effect of an electromagnetic field on natural convection in an inclined porous medium. Buoyancy-driven convection in a rectangular enclosure with a transverse magnetic field has been considered by Garandet et al. [19] and Khanafer and Chamkha [20].

In certain porous media applications, such as those involving heat removal from nuclear fuel debris, underground disposal of radioactive waste material, storage of foodstuffs, and exothermic chemical reactions and dissociating fluids in packed-bed reactors, the working fluid heat generation (source) or absorption (sink) effects are important. Representative studies dealing with these effects have been reported by such authors as Acharya and Goldstein [21], Vajravelu and Nayfeh [22], and Chamkha [23, 24]. The heat generation or absorption effects have been assumed to be either constant, space dependent, or temperature dependent. Since the difference between the free stream temperature and the temperature in the boundary layer may be large, a temperature-dependent heat source or sink is employed.

In this work we consider simultaneous heat and mass transfer by mixed convection from a semi-infinite vertical permeable surface embedded in a fluid-saturated porous medium and in the presence of surface blowing or suction, magnetic field effects, heat generation or absorption effects, and the porous medium inertia and thermal dispersion effects. This will be done for power law variations of both the wall temperature and concentration and also for power law variations of both the wall heat and mass fluxes.

PROBLEM FORMULATION

Consider steady, laminar coupled heat and mass transfer by mixed convection flow of an electrically conducting and heat generation or absorbing fluid over a semi-infinite permeable vertical plate embedded in a fluid-saturated porous

medium. The plate extends vertically in the x direction, while a magnetic field of uniform strength B_0 is applied in the y direction that is normal to the plate. The electrically conducting, heat generating or absorbing fluid is assumed to be Newtonian and has constant properties except the density in the buoyancy term of the balance of the linear momentum equation. Also, the porosity and the permeability of the porous medium are assumed to be constant. Both the fluid and the porous medium are assumed to be in local thermal equilibrium. Two conditions of prescribed wall temperature and concentration and prescribed wall heat and mass fluxes are considered. The wall temperature and concentration or the wall heat flux and mass flux are assumed to have power law variations with the vertical distance along the plate x. However, the temperature and concentration of the free stream are assumed to be constant. The temperature and concentration at the plate surface are always greater than the free stream values existing far from the plate surface. The magnetic Reynolds number is assumed to be so small that the induced magnetic field can be neglected. In addition, there is no applied electric field, and the Hall effect, Joule heating, and viscous dissipation are all neglected in this work.

The present investigation for mixed convection flow in porous media is based on Darcy's law. An important assumption for the validity of this law is that the free stream velocity is somewhat low. In the present work, the Reynolds number Re based on the pore size is assumed to be close to unity so that the porous medium inertia and thermal dispersion effects can be included without including the viscous term which becomes important for higher Re. The governing equations within the boundary layer taking into account the Boussinesq approximation may be written as follows:

$$\frac{\partial u}{\partial x} + \frac{\partial v}{\partial y} = 0 \tag{1}$$

$$\left(1 + \frac{\sigma B_0^2 K}{\rho \nu} + \frac{2FKu}{\rho \nu}\right) \frac{\partial u}{\partial y} = \frac{g\beta_T K}{\nu} \frac{\partial T}{\partial y} + \frac{g\beta_C K}{\nu} \frac{\partial C}{\partial y} \tag{2}$$

$$u\frac{\partial T}{\partial x} + v\frac{\partial T}{\partial y} = \frac{\partial}{\partial y}\left(\alpha_e \frac{\partial T}{\partial y}\right) + \frac{Q_0}{\rho c_p}(T - T_\infty) \tag{3}$$

$$u\frac{\partial C}{\partial x} + v\frac{\partial C}{\partial y} = D\frac{\partial^2 C}{\partial y^2} \tag{4}$$

where u, v, T, and C are the fluid x component of velocity, y component of velocity, temperature, and concentration, respectively; u and v are the Darcian velocities; ρ, ν, c_p, β_T, and β_C are the fluid density, kinematic viscosity, specific heat at constant pressure, coefficient of thermal expansion, and coefficient of concentration expansion, respectively; σ, Q_0, and D are the fluid electrical conductivity, heat generation (>0) or absorption (<0) coefficient, and mass diffusivity, respectively; g and B_0 are the gravitational acceleration and magnetic induction, respectively; and K, F, and α_e are the porous medium permeability, inertia coefficient, and effective thermal diffusivity, respectively.

The boundary conditions for the problem of power law variations of wall temperature and concentration can be written as

$$y = 0\text{: } v = V_w(x) \qquad T = T_w(x) = T_\infty + a_1 x^n \qquad C = C_w(x) = C_\infty + a_2 x^n \quad (5)$$

$$y \to \infty\text{: } u = u_\infty \qquad T = T_\infty \qquad C = C_\infty \quad (6)$$

However, for the problem of power law variations of wall heat and mass fluxes, Eqs. (5) are replaced by

$$y = 0\text{: } v = V_w(x) \qquad -k_e\left(\frac{\partial T}{\partial y}\right)\bigg|_{y=0} = b_1 x^m \qquad -D\left(\frac{\partial C}{\partial y}\right)\bigg|_{y=0} = b_2 x^m \quad (7)$$

In Eqs. (5)–(7), T_w and C_w are the wall temperature and concentration, respectively. V_w is the surface mass transfer coefficient; u_∞, T_∞, and C_∞ are the free stream velocity, temperature, and concentration, respectively; and a_1, a_2, b_1, b_2, m, and n are constants.

In situations of fluid flow and heat transfer in porous media, the effective thermal diffusivity is modeled by Yagi et al. [25] and later by Plumb [13] according to

$$\alpha_e = \alpha + \alpha_d \quad (8)$$

where α and α_d are the fluid molecular thermal diffusivity and the diffusivity of the porous medium due to thermal dispersion, respectively. Yagi et al. [25] and Plumb [13] represented α_d as a linear relation of the fluid velocity as follows:

$$\alpha_d = \gamma u d \quad (9)$$

where γ and d are a thermal dispersion constant and the porous medium particle diameter, respectively.

Power Law Variation of Wall Temperature and Concentration (PST/PSC)

We invoke the following dimensionless variables, which were reported earlier by Yih [12]:

$$\xi = \frac{\mathrm{Ra}_x}{\mathrm{Pe}_x} \quad (10)$$

$$\eta = \frac{y}{x}\,\mathrm{Pe}_x^{1/2} \quad (11)$$

$$f(\xi, \eta) = \frac{\psi}{\alpha\,\mathrm{Pe}_x^{1/2}} \quad (12)$$

$$\theta(\xi,\eta)=\frac{T-T_\infty}{T_w-T_\infty} \tag{13}$$

$$\phi(\xi,\eta)=\frac{C-C_\infty}{C_w-C_\infty} \tag{14}$$

where ψ is the dimensional stream function, $\mathrm{Ra}_x=g\beta_T K(T_w-T_\infty)x/(\nu\alpha)$ is the local Rayleigh number, and $\mathrm{Pe}_x=u_\infty x/\alpha$ is the local Péclet number. This results in the following nonsimilar equations

$$(1+M+\Gamma f')f''=\xi(\theta'+N\phi') \tag{15}$$

$$(1+D_s f')\theta''+\left(D_s f''+\frac{1}{2}f\right)\theta'+(\delta_T\xi^{1/n}-nf')\theta=n\xi\left(f'\frac{\partial\theta}{\partial\xi}-\theta'\frac{\partial f}{\partial\xi}\right) \tag{16}$$

$$\left(\frac{1}{\mathrm{Le}}\right)\phi''+\frac{1}{2}f\phi'-nf'\phi=n\xi\left(f'\frac{\partial\phi}{\partial\xi}-\phi'\frac{\partial f}{\partial\xi}\right) \tag{17}$$

where

$$M=\frac{\sigma B_0^2 K}{\rho\nu}\qquad \Gamma=\frac{2FKu_\infty}{\rho\nu}\qquad N=\frac{\beta_C(C_w-C_\infty)}{\beta_T(T_w-T_\infty)} \tag{18}$$

$$\mathrm{Le}=\frac{\alpha}{D}\qquad \delta_T=\frac{Q_0}{\rho c_p u_\infty}\left(\frac{\mathrm{Pe}_L}{\mathrm{Ra}_L}\right)^{1/n}\qquad D_s=\frac{\gamma u_\infty d}{\alpha} \tag{19}$$

are the square of the Hartmann number, dimensionless porous medium inertia coefficient, buoyancy ratio, Lewis number, dimensionless internal heat generation or absorption parameter, and porous medium thermal dispersion parameter, respectively. Q_0 is assumed constant for all values of $n>0$ except for $n=0$, where it must be proportional to $1/x$ in order to eliminate the singularity of Eq. (16) when $n=0$. Pe_L and Ra_L are the Péclet and Rayleigh numbers evaluated at the characteristic length of the vertical plate L.

After transformation, the boundary conditions become

$$\begin{aligned}&\eta=0\text{: } f=2V_0 \qquad \theta=1 \qquad \phi=1\\ &\eta\to\infty\text{: } f'=1 \qquad \theta=0 \qquad \phi=0\end{aligned} \tag{20}$$

where $V_0=V_w[x/(\alpha u_\infty)]^{1/2}$ is the dimensionless wall mass transfer coefficient. In order to eliminate x from the boundary conditions, the normal velocity at the surface V_w must be inversely proportional to the square root of x.

The local Nusselt and Sherwood numbers are important physical characteristics for this flow and heat transfer situation. These are defined as follows:

$$\mathrm{Nu}_x = \frac{hx}{k_e} = -\theta'(\xi, 0)\mathrm{Pe}_x^{1/2} \tag{21}$$

$$\mathrm{Sh}_x = \frac{h_m x}{D} = -\phi'(\xi, 0)\mathrm{Pe}_x^{1/2} \tag{22}$$

where h, k_e, and h_m are the convective heat transfer coefficient, effective thermal conductivity, and convective mass transfer coefficient, respectively.

Power Law Variation of Wall Heat and Mass Fluxes (PHF/PMF)

For this situation, we use the following dimensionless variables, which were reported earlier by Yih [12]:

$$\xi = \frac{\mathrm{Ra}_x^*}{(\mathrm{Pe}_x)^{1/2}} \tag{23}$$

$$\eta = \frac{y}{x}\mathrm{Pe}_x^{1/2} \tag{24}$$

$$f(\xi, \eta) = \frac{\psi}{\alpha \mathrm{Pe}_x^{1/2}} \tag{25}$$

$$\theta(\xi, \eta) = \frac{(T - T_\infty) k \mathrm{Pe}_x^{1/2}}{q_w(x)\, x} \tag{26}$$

$$\phi(\xi, \eta) = \frac{(C - C_\infty) D \mathrm{Pe}_x^{1/2}}{m_w(x)\, x} \tag{27}$$

where $\mathrm{Ra}_x^* = g\beta_T K q_w x^2/(\nu\alpha k)$ is the modified local Rayleigh number and q_w and m_w are wall heat and mass fluxes, respectively. Using these variables to transform Eqs. (2)–(7) results in the following nonsimilar equations:

$$(1 + M + \Gamma f')f'' = \xi(\theta' + N^*\phi') \tag{28}$$

$$(1 + D_s f')\theta'' + \left(D_s f'' + \frac{1}{2}f\right)\theta' + \left[\delta_Q \xi^{2/(3+2m)} - \left(m + \frac{1}{2}\right)f'\right]\theta = \left(m + \frac{1}{2}\right)\xi\left(f'\frac{\partial\theta}{\partial\xi} - \theta'\frac{\partial f}{\partial\xi}\right) \tag{29}$$

$$\left(\frac{1}{\mathrm{Le}}\right)\phi'' + \frac{1}{2}f\phi' - \left(m + \frac{1}{2}\right)f'\phi = \left(m + \frac{1}{2}\right)\xi\left(f'\frac{\partial\phi}{\partial\xi} - \phi'\frac{\partial f}{\partial\xi}\right) \tag{30}$$

where M, Γ, Le, and D_s are the same as defined for the previous variations of the wall temperature and concentration and

$$N^* = \frac{\beta_C m_w / D}{\beta_T q_w / k} \tag{31}$$

$$\delta_Q = \frac{Q_0}{\rho c_p u_\infty} \left(\frac{\mathrm{Pe}_L}{\mathrm{Ra}_L^{*2}} \right)^{1/(3+2m)} \tag{32}$$

are buoyancy ratio and the dimensionless internal heat generation or absorption parameter for this case, respectively. Q_0 is assumed constant for all values of $m > -3/2$. However, for $m = -3/2$, Q_0 must be proportional to $1/x$ in order to eliminate the singularity associated with Eq. (29) when $m = -3/2$. Ra_L^* is the modified Rayleigh number evaluated at $x = L$.

The boundary conditions after transformation for this case become

$$\eta = 0: \; f = 2V_0 \qquad \theta' = -1 \qquad \phi' = -1 \tag{33}$$

$$\eta \to \infty: \; f' = 1 \qquad \theta = 0 \qquad \phi = 0 \tag{34}$$

where the dimensionless wall mass transfer coefficient V_0 is defined as before. Again, to eliminate x from the boundary conditions, the normal velocity at the surface V_w must be inversely proportional to the square root of x.

For this case, the local Nusselt and Sherwood numbers are given by

$$\mathrm{Nu}_x = \frac{hx}{k_e} = \frac{1}{\theta(\xi, 0)} \mathrm{Pe}_x^{1/2} \tag{35}$$

$$\mathrm{Sh}_x = \frac{h_m x}{D} = \frac{1}{\phi(\xi, 0)} \mathrm{Pe}_x^{1/2} \tag{36}$$

NUMERICAL METHOD

The implicit finite difference method discussed by Blottner [26] has proven to be successful at producing accurate solutions for differential equations similar to Eqs. (15)–(21) and Eqs. (28)–(34). Therefore it is employed in the present work. These equations have been linearized and then discretized using three-point central difference quotients with variable step sizes in the η direction. The resulting equations form a tridiagonal system of algebraic equations that are solved by the well-known Thomas algorithm (see [26]). Because of the nonlinearities of the equations, an iterative solution is required. A backward-difference approximation of all first-order derivatives with respect to ξ is used to evaluate the solution at the next line of constant ξ using the known solution at the previous line. Therefore the solution marches from $\xi = 0$ (where the equations become similar) toward a predetermined value of ξ. For convergence, the maximum absolute error

between two successive iterations was taken to be 10^{-7}. A starting step size of 0.001 in the η direction with an increase of 1.015 times the previous step size was found to give accurate results. The total number of points in the η direction was taken to be 499 to ensure a proper approach of the solution to the free stream conditions. The accuracy of the aforementioned numerical method was validated by direct comparisons with the numerical results reported earlier by Yih [12] for the cases of $D_s = 0$ and in the absence of magnetic heat generation or absorption and wall blowing or suction effects. Table 1 presents the results of these comparisons for the prescribed wall temperature condition, whereas Table 2 reports the comparisons for the prescribed wall heat flux condition. It can be seen from these

Table 1. Comparisons of the values of $-\theta'(\xi,0)$ for various values of ξ and n with $D_s = 0$, Le $= 1.0$, $M = 0$, $N = 0$, $V_0 = 0$, and $\delta_T = 0$

	$n = 0.0$			$n = 0.5$			$n = 1.0$		
ξ	Hsieh et al. [8]	Yih [12]	Present method	Hsieh et al. [8]	Yih [12]	Present method	Hsieh et al. [8]	Yih [12]	Present method
0.0	0.5642	0.5642	0.5644	0.8862	0.8862	0.8861	1.1284	1.1284	1.1280
0.5	0.6474	0.6474	0.6476	1.0428	1.0428	1.0416	1.3339	1.3339	1.3318
1.0	0.7206	0.7206	0.7209	1.1780	1.1779	1.1763	1.5109	1.5108	1.5080
10	1.5163	1.5162	1.5171	2.5960	2.5959	2.5935	3.3591	3.3590	3.3534
20	2.0665	2.0663	2.0675	3.5602	3.5534	3.5561	4.6128	4.6022	4.6035
30	2.4981	2.4979	2.4994	4.3140	4.3148	4.3079	5.5924	5.5922	5.5490
40	2.8665	2.8651	2.8669	4.9545	4.9539	4.9462	6.4244	6.4240	6.4067
50	3.1909	3.1903	3.1923	5.5212	5.5204	5.5106	7.1605	7.1604	7.1383
100	4.4763	4.4748	4.4777	7.7570	7.7556	7.7348	10.063	10.063	10.019
500	9.9555	9.9392	9.9463	17.264	17.248	17.1366	22.389	22.388	22.157
1000	14.090	14.044	14.055	24.419	24.377	24.149	31.643	31.643	31.177

Table 2. Comparisons of the values of $1/\theta(\xi,0)$ for various values of ξ and m with $D_s = 0$, Le $= 1.0$, $M = 0$, $N^* = 0$, $V_0 = 0$, and $\delta_Q = 0$

	$m = -0.5$			$m = 0.0$			$m = 1.0$		
ξ	Hsieh et al. [8]	Yih [12]	Present method	Hsieh et al. [8]	Yih [12]	Present method	Hsieh et al. [8]	Yih [12]	Present method
0.0	0.5642	0.5642	0.5644	0.8863	0.8862	0.8861	1.3294	1.3293	1.3287
0.5	0.6825	0.6825	0.6827	1.0099	1.0099	1.0024	1.4579	1.4579	1.4505
1.0	0.7625	0.7625	0.7628	1.1017	1.1017	1.0925	1.5601	1.5601	1.5500
10	1.3401	1.3408	1.3413	1.8252	1.8247	1.8194	2.4386	2.4380	2.4281
20	1.6482	1.6489	1.6495	2.2245	2.2123	2.2201	2.9425	2.9254	2.9332
30	1.8680	1.8687	1.8695	2.5114	2.5049	2.5203	3.3074	3.2958	3.2988
40	2.0445	2.0452	2.0460	2.7425	2.7372	2.7390	3.6023	3.5928	3.6074
50	2.1942	2.1949	2.1958	2.9389	2.9349	2.9355	3.8537	3.8459	3.8570
100	2.7411	2.7414	2.7425	3.6581	3.6558	3.6546	4.7768	4.7718	4.7680
500	4.6298	4.6416	4.6436	6.1234	6.1572	6.1564	8.0165	7.9706	7.9824
1000	5.8361	5.8369	5.8394	7.7150	7.7385	7.7369	10.063	10.023	10.026

tables that there is excellent agreement between the results. These favorable comparisons lend confidence in the numerical results to be reported in the next section.

RESULTS AND DISCUSSION

Figure 1 illustrates the effects of the square of the Hartmann number M and the mixed convection variable ξ on the local Nusselt number $\mathrm{Nu}\,\mathrm{Pe}_x^{-1/2}$ for uniform wall temperature and concentration. The presence of a magnetic field in an electrically conducting fluid has the effect of reducing the flow due to the resulting resistance magnetic force, which is called the Lorentz force. In addition, the flow temperature increases as the magnetic field strength increases, causing the wall slope of the temperature profile to increase. This results in decreasing local Nu, as shown in Figure 1. A very similar trend was observed for the case of uniform heat flux in which the wall temperature increased and the local Nu decreased as the magnetic field strength was increased. For this reason, no figures are shown for this case.

Figure 2 depicts the influence of the porous medium thermal dispersion parameter D_s and the mixed convection variable ξ on the local Nu for the uniform wall temperature and concentration condition. Increasing the thermal dispersion parameter results in an increase in the thermal diffusion, and as a result, the flow velocity along the plate increases. This, in turn, results in increasing the rate of heat extracted from the plate. This does not require an increase in the local Nu, since the effective thermal conductivity at the wall is also increased as a result of thermal diffusion. Therefore the local Nu decreases as D_s increases, as shown in Figure 2. The same effect was observed for the case of uniform wall heat and mass fluxes in which the local Nu decreased as D_s was increased.

Figures 3 and 4 show the effects of the dimensionless internal heat generation or absorption parameter δ_T (for prescribed wall temperature) and δ_Q (for prescribed wall heat flux) and ξ with $m = n = 1.0$ on the local Nu, respectively. As

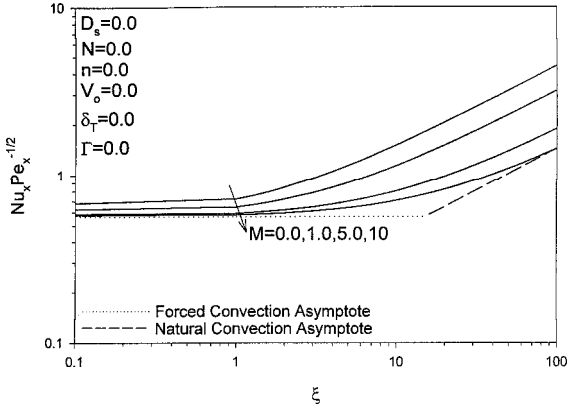

Figure 1. Effects of M and ξ on the Nusselt number (PST/PSC).

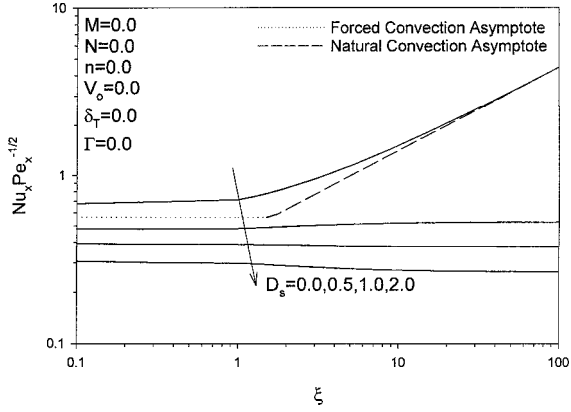

Figure 2. Effects of D_s and ξ on the Nusselt number (PST/PSC).

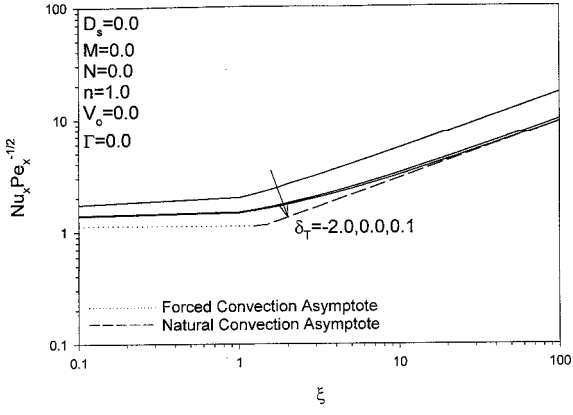

Figure 3. Effects of δ_T and ξ on the Nusselt number (PST/PSC).

δ_T and δ_Q increase, the flow temperatures increase, resulting in decrease in the absolute slope of the temperature profile at the wall for the prescribed wall temperature condition, and increase in the wall temperature for the prescribed wall heat flux condition. This has the direct effect of reducing the local Nu for both thermal conditions, as is clear from Figures 3 and 4. It should be mentioned that for values of $\delta_T > 0.1$ and $\delta_Q > 0$, convergence difficulties were encountered. For this reason, no results associated with these conditions are presented in Figures 3 and 4.

Figures 5 and 6 illustrate the effects of the power index n (for prescribed wall temperature) and m (for prescribed wall heat flux) and ξ on the local Nu, respectively. As n and m increase, the temperature gradients along the x direction are expected to increase. This, in turn, results in increasing the convective heat transfer rate. Therefore the local Nu increases for both thermal conditions as shown in Figures 5 and 6.

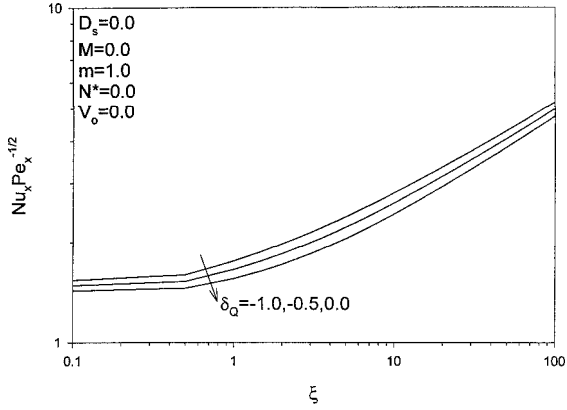

Figure 4. Effects of δ_Q and ξ on the Nusselt number (PHF/PMF).

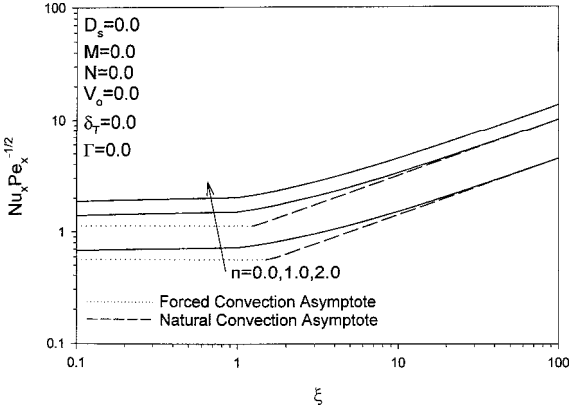

Figure 5. Effects of n and ξ on the Nusselt number (PST/PSC).

Figure 7 presents the effects of the buoyancy ratio N (for prescribed wall temperature) and ξ on the local Nu. Increasing the value of N results in increase of the buoyancy effects, causing higher flow velocities. This causes increases in the absolute wall temperature slope, which produces increases in local Nu, as is evident from Figure 7. Nu for the case of prescribed wall heat flux showed a similar trend, in which it increased as the buoyancy ratio N^* was increased. For the same reason mentioned above, the local Sh also increases as N or N^* increases, since the energy and concentration equations are similar.

Figures 8 and 9 show the influence of the dimensionless blowing or suction parameter V_0 and ξ on the local Nu for both uniform wall temperature and wall heat flux conditions, respectively. Wall fluid suction ($V_0 > 0$) has the effect of reducing the velocity and thermal boundary layer thicknesses. Consequently, the rate of heat transfer increases. On the other hand, wall fluid injection or blowing produces the opposite effect, namely, a decrease in the wall heat transfer rate.

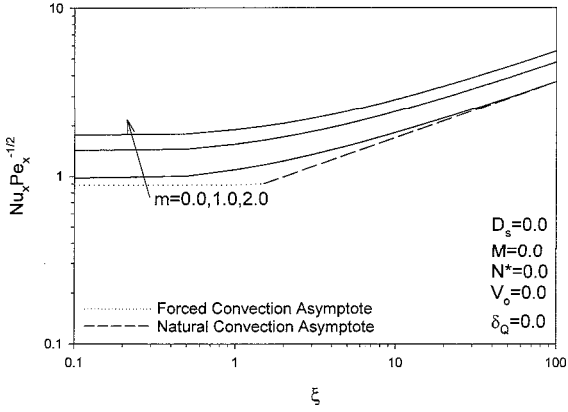

Figure 6. Effects of m and ξ on the Nusselt number (PHF/PMF).

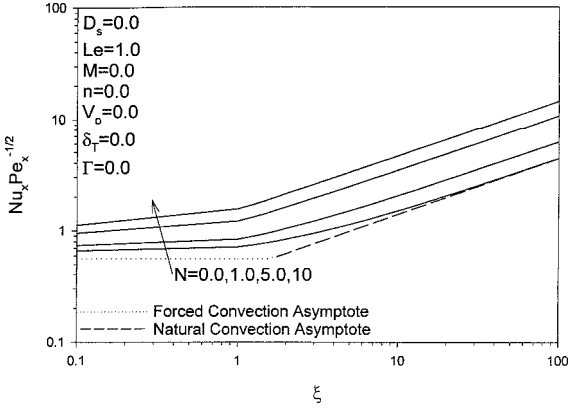

Figure 7. Effects of N and ξ on the Nusselt number (PST/PSC).

These behaviors are illustrated by the increase of the local Nu in Figures 8 and 9 as V_0 increases. It should be noticed that the suction/injection parameter V_0 has a greater effect in the forced-convection-dominated region for the uniform heat flux case than its counterpart for the case of an isothermal wall.

Figures 10–12 display the effects of the Lewis number Le and ξ on the local Nu and Sh for both previously mentioned uniform thermal conditions. Increases in the values of Le result in decreases in the mass diffusivity. This, in turn, results in decrease in the concentration buoyancy forces and therefore the flow velocity. Consequently, local Nu decreases as shown in Figures 10 and 12. By comparing Figures 10 and 12, it can be seen that Le has a greater effect on Nu for the case of uniform heat flux than that for the isothermal surface, especially in the free or natural-convection-dominated region. As expected, increasing the value of Le produces lower concentrations, which result in increasing the local Sh, as shown in Figure 11 for the uniform wall temperature case. It should be mentioned that in all

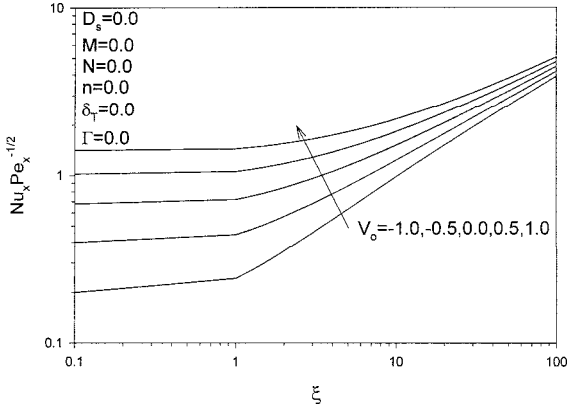

Figure 8. Effects of V_0 and ξ on the Nusselt number (PST/PSC).

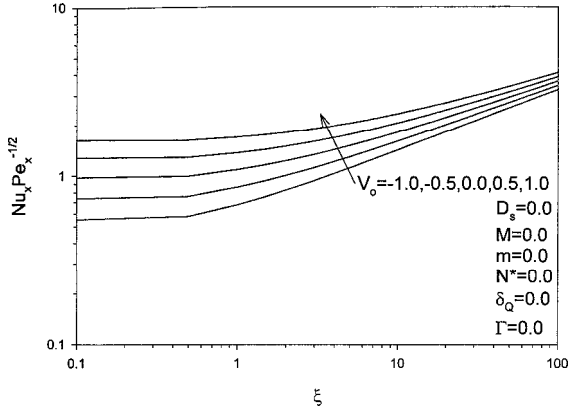

Figure 9. Effects of V_0 and ξ on the Nusselt number (UHF/UMF).

of the above studied cases, forced and natural convection asymptotes are realized except for the cases where internal heat generation or absorption effects are present, since their presence does not produce similar equations as $\xi \to \infty$. These asymptotes were obtained by using the derived expressions reported by Yih [12].

Tables 3 and 4 show the influence of the dimensionless porous medium inertia coefficient Γ and the thermal dispersion parameter D_s on the local Nu for both uniform wall temperature and heat flux, respectively. Additional resistance against the flow is introduced because of the porous medium inertia effect. This results in decreasing the enthalpy of the flow streams for both uniform wall temperature and heat flux conditions. Thus the local Nu for both conditions decreases when Γ increases, as shown in Tables 3 and 4. It should be noted that the inertia of the porous medium produces no effect for the case of forced convection ($\xi = 0$). This is because the model of the problem does not take into account the no-slip velocity boundary conditions.

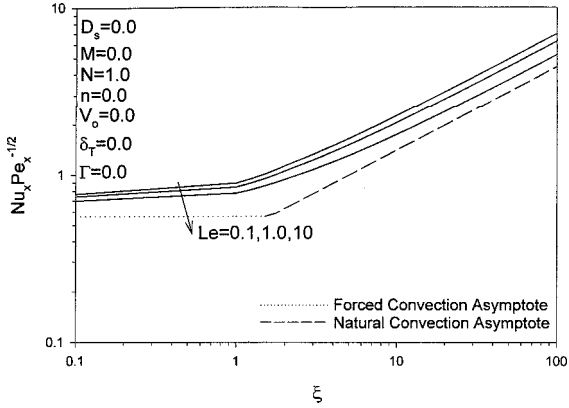

Figure 10. Effects of Le and ξ on the Nusselt number (PST/PSC).

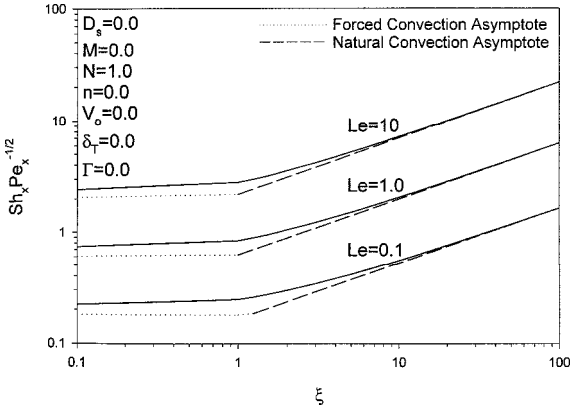

Figure 11. Effects of Le and ξ on the Sherwood number (PST/PSC).

The following correlations are obtained for local Nu as a function of the mixed convection variable ξ with all of M, m, N or N^*, n, V_0, and δ_T or δ_Q set to zero for both uniform wall temperature and uniform heat flux conditions, respectively:

$$\mathrm{Nu}_x \mathrm{Pe}_x^{-1/2} = 0.5335 + 0.2887\xi^{0.5645} \tag{37}$$

$$\mathrm{Nu}_x \mathrm{Pe}_x^{-1/2} = 0.8727 + 0.3467\xi^{0.4538} \tag{38}$$

Both correlations are valid for $0 \leqslant \xi \leqslant 100$ with maximum errors for both correlations about 10%. It is seen from Eqs. (37) and (38) that Nu has an increasing behavior with ξ for both uniform wall temperature and heat flux cases and that this behavior is less pronounced in the forced-convection-dominated region ($0 \leqslant \xi \leqslant 1$) than in the natural-convection-dominated region ($\xi > 1$). This trend was clearly observed in almost all the figures presented in the previous section.

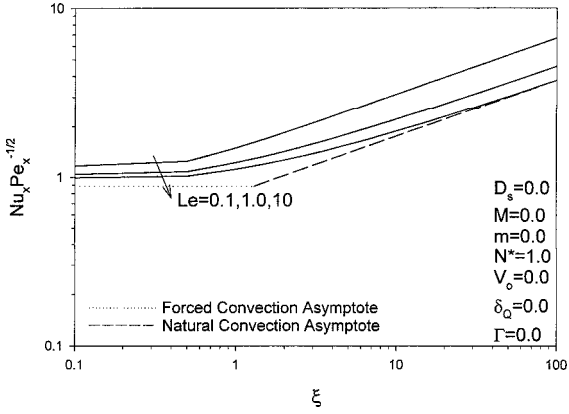

Figure 12. Effects of Le and ξ on the Nusselt number (UHF/UMF).

Table 3. Effects of D_s and Γ on $-\theta'(\xi,0)$ for uniform wall temperature condition with $M=0$, $N=0$, $V_0=0$, and $\delta_T=0$

ξ	$D_s=0.0$ and $\Gamma=0.0$	$D_s=0.0$ and $\Gamma=0.5$	$D_s=0.5$ and $\Gamma=0.5$
0	0.5652	0.5652	0.4609
1	0.7209	0.6659	0.4822
5	1.1462	0.9109	0.5197
10	1.5171	1.0933	0.5397
50	3.1923	1.7189	0.5799
100	4.4777	2.0838	0.5924

Table 4. Effects of D_s and Γ on $1/\theta(\xi,0)$ for uniform wall heat flux condition with $M=0$, $N=0$, $V_0=0$, and $\delta_Q=0$

ξ	$D_s=0.0$ and $\Gamma=0.0$	$D_s=0.0$ and $\Gamma=0.5$	$D_s=0.5$ and $\Gamma=0.5$
0	0.8861	0.8861	0.7235
1	1.0810	1.0234	0.7820
5	1.5052	1.3104	0.8706
10	1.8125	1.5059	0.9129
50	2.9330	2.1369	0.9942
100	3.6530	2.4903	1.0189

CONCLUSION

We considered the problem of steady, laminar, simultaneous heat and mass transfer by mixed convection boundary layer flow of an electrically conducting and heat generating or absorbing fluid over a permeable vertical plate embedded in a uniform porous medium with thermal dispersion. Both the wall temperature and concentration and the wall heat and mass fluxes were assumed to vary with the

vertical distance along the plate according to a power law form. Also, a transverse magnetic field of uniform strength was assumed to exist in the direction normal to that of the flow. Nonsimilar governing equations were obtained by using previously reported transformations. These transformed equations were then solved numerically by an accurate implicit, iterative, finite difference scheme. Excellent agreements were obtained between the present results and those of previously published work for special cases of the problem. It was found that for both prescribed wall temperature and concentration conditions and prescribed wall heat flux and mass flux conditions while local Nu decreased as a result of the presence of either the magnetic field or positive surface blowing, it increased due to imposition of both surface suction and larger values of power law indices. Also, Nu was increased due to the presence of heat absorption effects. Furthermore, increasing the ratio of concentration to thermal buoyancies was found to cause enhancements in the values of Nu and Sh. Finally, porous medium inertia and thermal dispersion effects were found to decrease local Nu. It is hoped that the present work will serve as a vehicle for understanding more complex problems involving the various physical effects investigated in the present problem.

REFERENCES

1. M. Karimi-Fard, M. C. Charrier-Mojtabi, and K. Vafai, Non-Darcian Effects on Double-Diffusive Convection Within a Porous Medium, *Numer. Heat Transfer Part A*, vol. 31, pp. 837–852, 1997.
2. K. Vafai and C. L. Tien, Boundary and Inertia Effects on Flow and Heat Transfer in Porous Media, *Int. J. Heat Mass Transfer*, vol. 24, pp. 195–203, 1981.
3. A. Amiri and K. Vafai, Analysis of Dispersion Effects and Non-Thermal Equilibrium, Non-Darcian, Variable Porosity Incompressible Flow Through Porous Media, *Int. J. Heat Mass Transfer*, vol. 37, pp. 936–954, 1994.
4. P. Cheng and W. J. Minkowycz, Free Convection About a Vertical Flat Plate Embedded in a Porous Medium with Application to Heat Transfer from a Dike, *J. Geophys. Res.*, vol. 82, pp. 2040–2044, 1977.
5. P. Ranganathan and R. Viskanta, Mixed Convection Boundary Layer Flow Along a Vertical Surface in a Porous Medium, *Numer. Heat Transfer*, vol. 7, pp. 305–317, 1984.
6. W. J. Minkowycz, P. Cheng, and C. H. Chang, Mixed Convection About a Nonisothermal Cylinder and Sphere in a Porous Medium, *Numer. Heat Transfer*, vol. 8, pp. 349–359, 1985.
7. A. Nakayama and H. Koyama, A General Similarity Transformation for Free, Forced and Mixed Convection Flows Within a Fluid-Saturated Porous Medium, *J. Heat Transfer*, vol. 109, pp. 1041–1045, 1987.
8. J. C. Hsieh, T. S. Chen, and B. F. Armaly, Non-Similarity Solutions for Mixed Convection from Vertical Surfaces in a Porous Medium: Variable Temperature or Heat Flux, *Int. J. Heat Mass Transfer*, vol. 36, pp. 1485–1493, 1993.
9. R. S. Gorla, A. Y. Bakir, and L. Byrd, Effects of Thermal Dispersion and Stratification on Combined Convection on a Vertical Surface Embedded in a Porous Medium, *Transport Porous Media*, vol. 25, pp. 275–282, 1996.
10. A. J. Chamkha, Hydrodynamic Natural Convection from an Isothermal Inclined Surface Adjacent to a Thermally Stratified Porous Medium, *Int. J. Eng. Sci.*, vol. 35, pp. 975–986, 1997.

11. F. C. Lai, Coupled Heat and Mass Transfer by Mixed Convection from a Vertical Plate in a Saturated Porous Medium, *Int. Commun. Heat Mass Transfer*, vol. 18, pp. 93–106, 1991.
12. K. A. Yih, Coupled Heat and Mass Transfer in Mixed Convection over a Vertical Flat Plate Embedded in Saturated Porous Media: PST/PSC or PHF/PMF, *Heat Mass Transfer*, vol. 34, pp. 55–61, 1998.
13. O. A. Plumb, Thermal Dispersion in Porous Media Heat Transfer, *ASME / JSME Thermal Conf. Proc.*, vol. 2, pp. 17–21, 1983.
14. J. T. Hong and C. L. Tien, Analysis of Thermal Dispersion Effect on Vertical-Plate Natural Convection in Porous Media, *Int. J. Heat Mass Transfer*, vol. 30, pp. 143–150, 1987.
15. P. Cheng and D. Vortmeyer, Transverse Thermal Dispersion and Wall Channeling in a Packed Bed with Forced Convective Flow, *Chem. Eng. Sci.*, vol. 43, pp. 2523–2532, 1988.
16. A. Rapits, C. Massias, and G. Tzivanidis, Hydromagnetic Free Convection Flow Through a Porous Medium Between Two Parallel Plates, *Phys. Lett.*, vol. 90A, pp. 288–289, 1982.
17. T. K. Aldoss, M. A. Al-Nimr, M. A. Jarrah, and B. J. Al-Sha'er, Magnetohydrodynamic Mixed Convection from a Vertical Plate Embedded in a Porous Medium, *Numer. Heat Transfer*, vol. 28A, pp. 635–645, 1995.
18. W. Bian, P. Vasseur, E. Belgin, and F. Meng, Effect of an Electromagnetic Field on Natural Convection in an Inclined Porous Medium, *Int. J. Heat Fluid Flow*, vol. 17, pp. 36–44, 1996.
19. J. P. Garandet, T. Alboussiere, and R. Moreau, Driven Convection in a Rectangular Enclosure with a Transverse Magnetic Field, *Int. J. Heat Mass Transfer*, vol. 34, pp. 741–748, 1992.
20. K. Khanafer and A. J. Chamkha, Hydrodynamic Natural Convection from an Inclined Porous Square Enclosure with Heat Generation, *Numer. Heat Transfer*, vol. 33, pp. 891–910, 1998.
21. S. Acharya and R. J. Goldstein, Natural Convection in an Externally Heated Vertical or Inclined Square Box Containing Internal Energy Sources, *ASME J. Heat Transfer*, vol. 107, pp. 855–866, 1985.
22. K. Vajravelu and J. Nayfeh, Hydromagnetic Convection at a Cone and a Wedge, *Int. Commun. Heat Mass Transfer*, vol. 19, pp. 701–710, 1992.
23. A. J. Chamkha, Non-Darcy Hydrodynamic Free Convection from a Cone and a Wedge in Porous Media, *Int. Commun. Heat Mass Transfer*, vol. 23, pp. 875–887, 1996.
24. A. J. Chamkha, Non-Darcy Fully Developed Mixed Convection in a Porous Medium Channel with Heat Generation/Absorption and Hydromagnetic Effects, *Numer. Heat Transfer*, vol. 32, pp. 853–875, 1997.
25. S. Yagi, D. Kunii, and K. Endo, Porous Media Heat Transfer, *Int. J. Heat Mass Transfer*, vol. 7, pp. 333–339, 1964.
26. F. G. Blottner, Finite-Difference Methods of Solution of the Boundary-Layer Equations, *AIAA J.*, vol. 8, pp. 193–205, 1970.